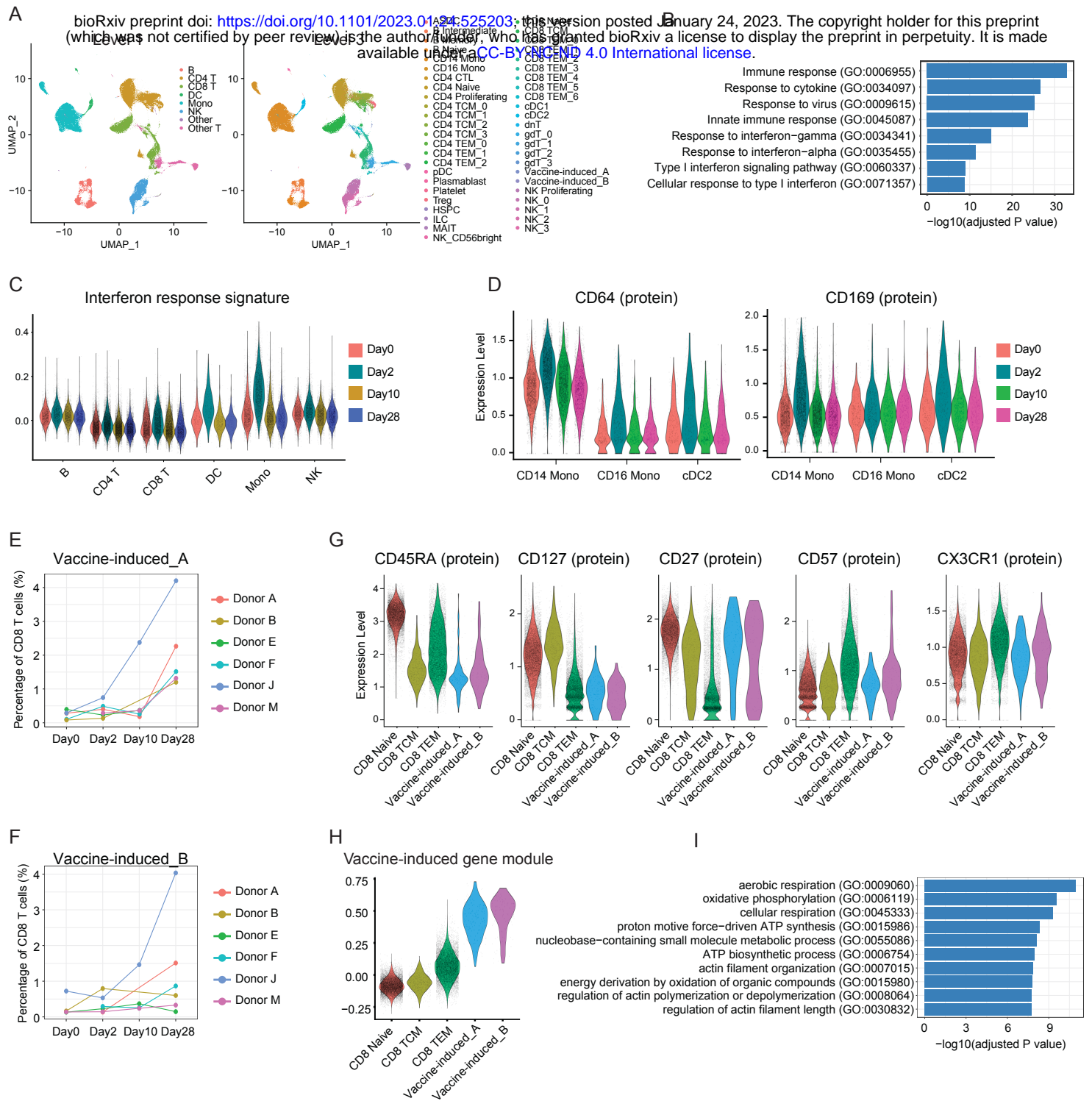


Supplementary Figure 1

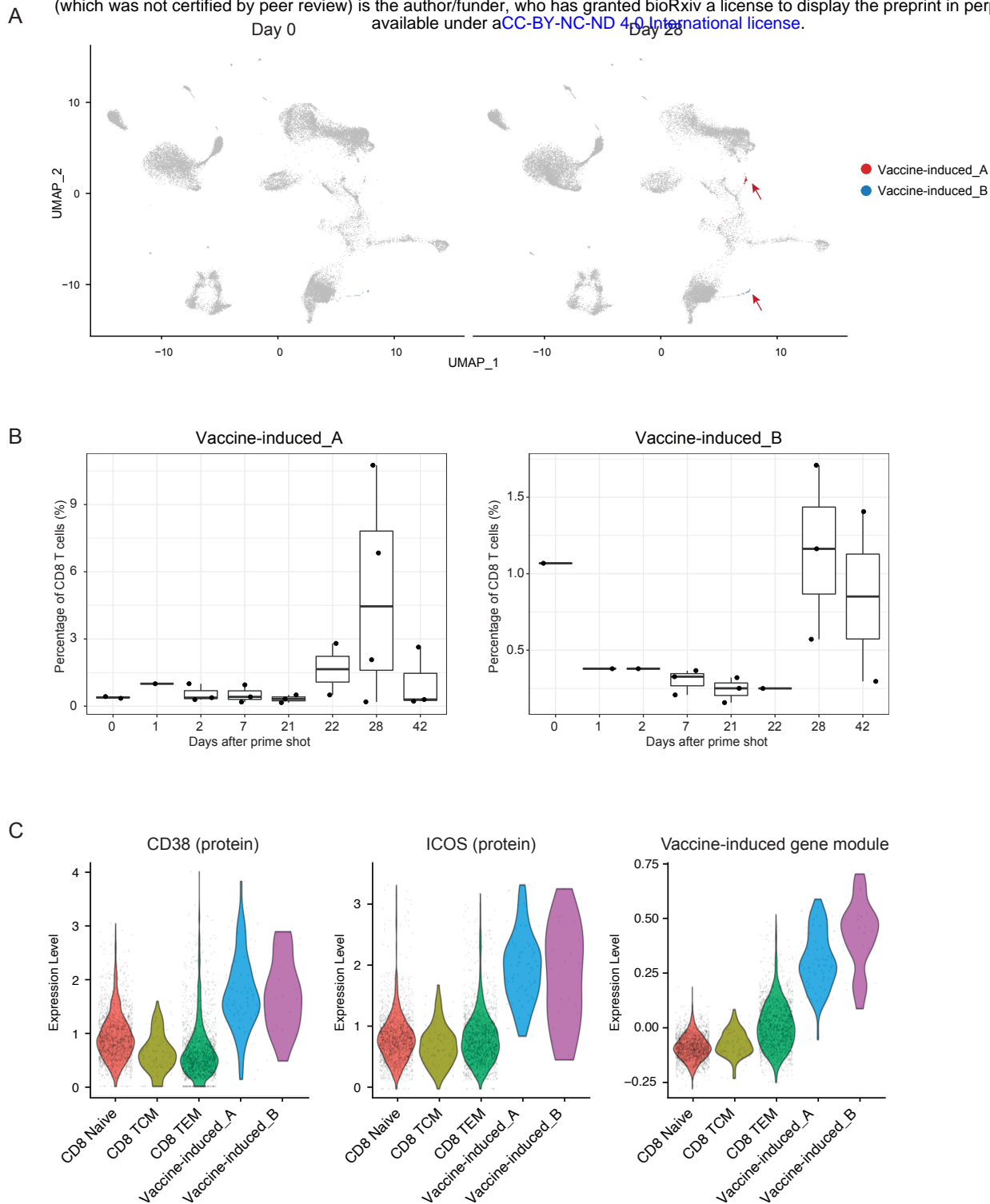


Supplementary Figure 1

(A) UMAP visualizations of 113,897 single cells profiled with CITE-seq and clustered on the weighted combination of both RNA and protein modalities. Cells are colored with either level 1 or level 3 annotations. (B) Enriched GO terms for activated (Day 2 vs Day 0) genes in CD14+ Monocytes. (C) Violin plots of interferon response signatures in selected cell types across four timepoints. (D) Violin plots of protein upregulation of CD64 and CD169 in single cells in selected cell types, across four timepoints. (E-F) Percentage of CD8+ T cells in vaccine-induced groups for each donor across four timepoints. (G) Violin plots showing the protein expression of CD45RA, CD127, CD27, CD57 and CXCR3R1 in selected cell types. (H) Violin plots comparing upregulated gene module scores in vaccine-induced group A and B cells, as well as selected other subsets. (I) Enriched GO terms for the 197 signature vaccine-induced gene set.

Supplementary Figure 2

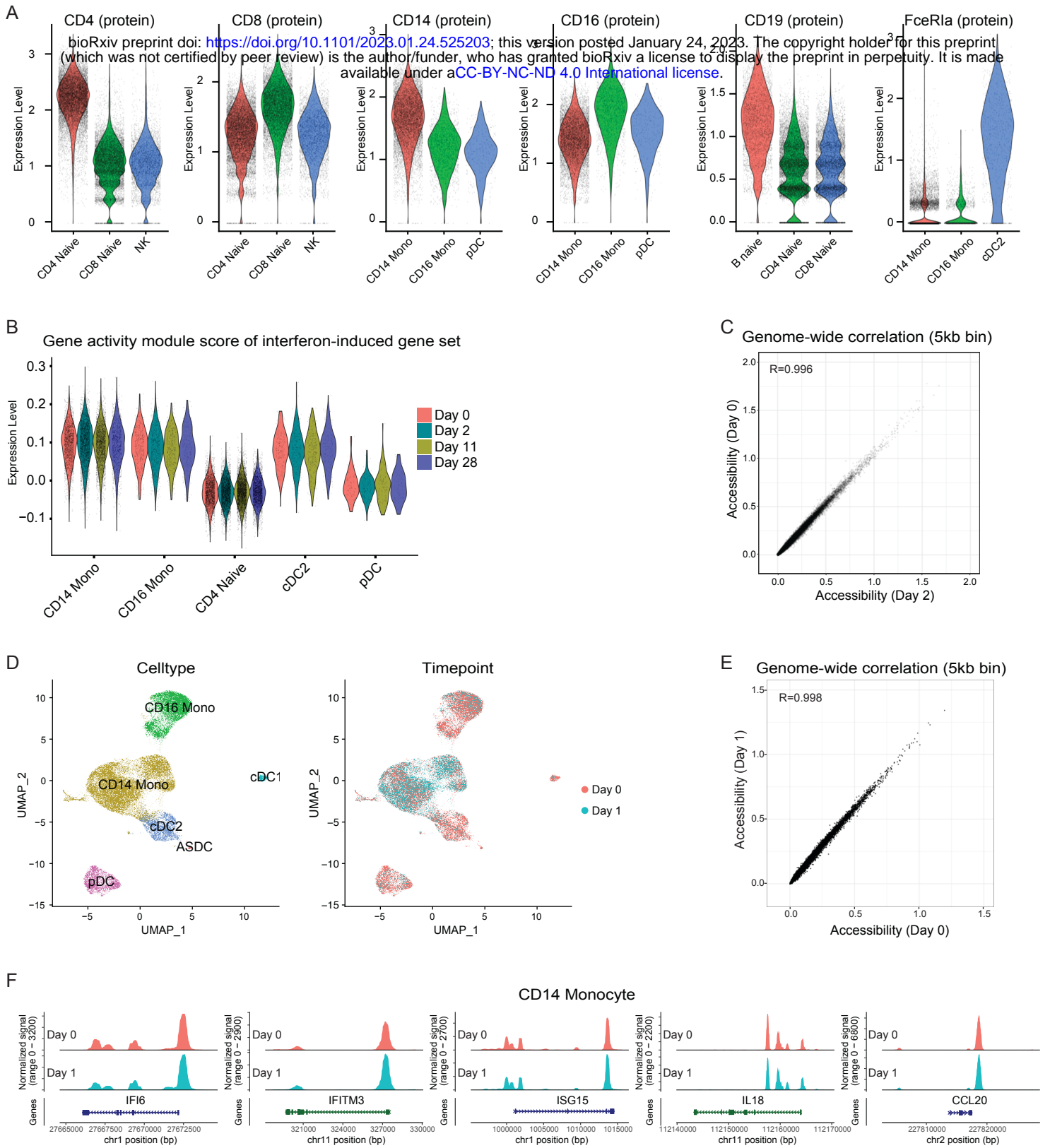
bioRxiv preprint doi: <https://doi.org/10.1101/2023.01.24.525203>; this version posted January 24, 2023. The copyright holder for this preprint (which was not certified by peer review) is the author/funder, who has granted bioRxiv a license to display the preprint in perpetuity. It is made available under a [CC-BY-NC-ND 4.0 International license](#).



Supplementary Figure 2

(A) UMAP visualization of CITE-seq data derived from human PBMC from Arunachalam et al. on Day0 and Day28, after reference mapping to the CITE-seq data in Figure 1B. Cells matching gene signature for vaccine-induced group A and B cells are highlighted in red and blue. **(B)** Boxplots showing the percentage of CD8+ T cells that fall in vaccine-induced group A (left) or group B cells (right) for each donor across eight timepoints. Each dot represents one donor. **(C)** Violin plots showing protein expression of CD38 and ICOS, along with a gene module score for vaccine-induced cells in selected CD8+ T cell subsets.

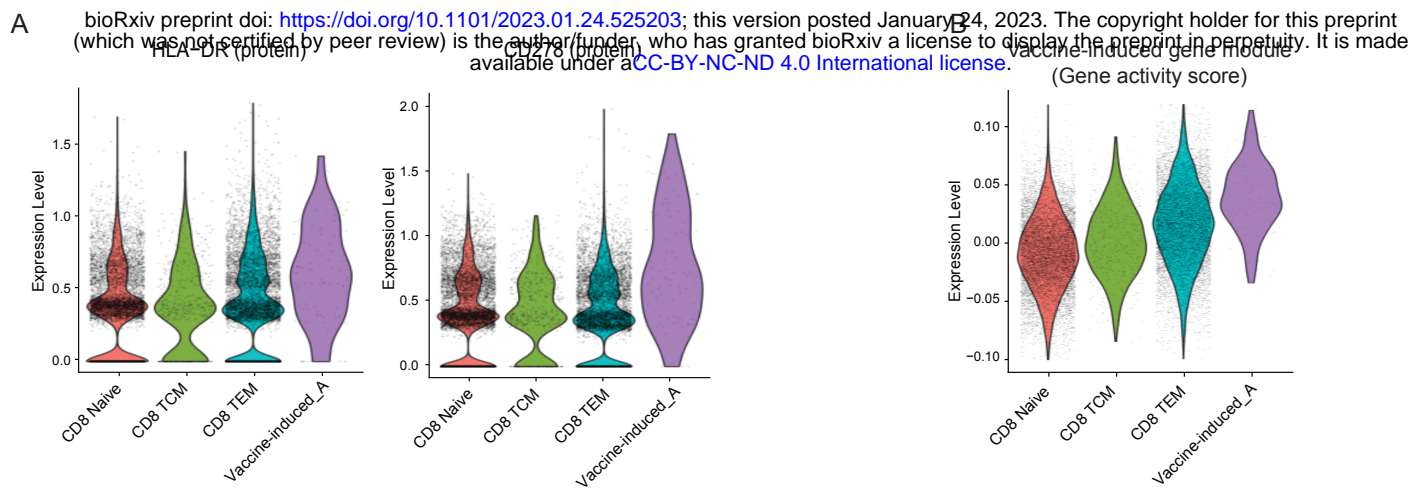
Supplementary Figure 3



Supplementary Figure 3

(A) Violin plots showing the expression of canonical surface proteins in the ASAP-seq dataset. Cells are grouped by bridge integration-derived labels. Proteins visualized include markers of CD4 and CD8 T cells, CD14 and CD16 monocytes, B cells and cDC2 cells. **(B)** Violin plots showing the gene ‘activity scores’, which are derived from scATAC-seq data, of the interferon-induced gene set shown in Figure 1C. **(C)** Scatter plot showing the correlation between pseudobulk chromatin accessibility of CD14 monocytes from Day 0 and Day 2 samples. Each point corresponds to a 5KB genomic bin. **(D)** UMAP visualization of the scATAC-seq profiles of myeloid cells from a trivalent inactivated seasonal influenza vaccine (TIV) study. Cells are colored by annotations (Left) or timepoints (right). **(E)** Scatter plot showing the correlation comparing pseudobulk chromatin accessibility of CD14 monocytes in the TIV dataset between Day 0 and Day 1. Each point corresponds to a 5KB genomic bin. **(F)** Visualization of open chromatin accessibility at representative loci on Day 0 and Day 1 in CD14 monocytes from the TIV study. Despite extensive transcriptional activation at these genes on Day 1, chromatin accessibility patterns do not change.

Supplementary Figure 4

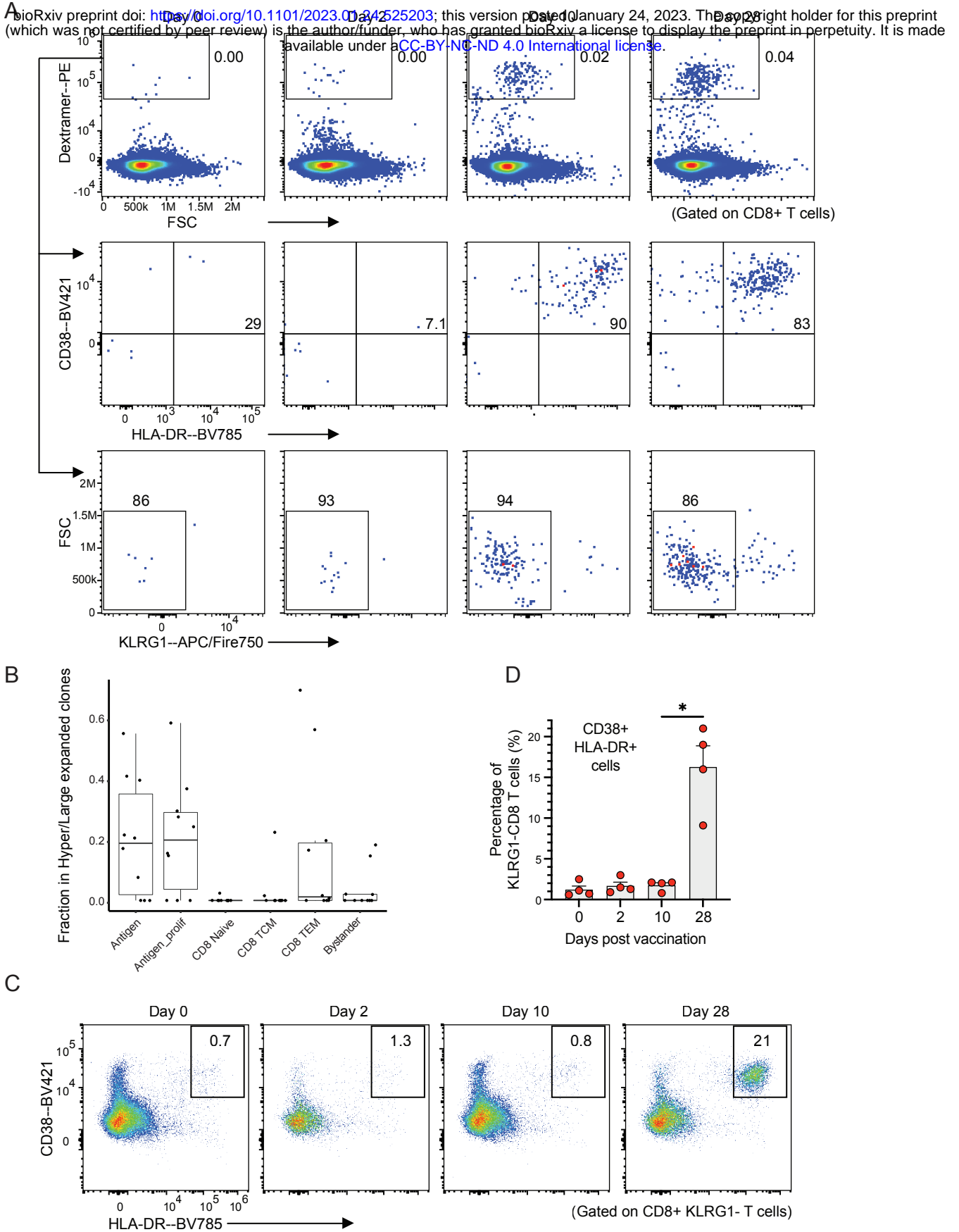


Supplementary Figure 4

(A) Violin plots showing the protein upregulation of HLA-DR and CD278 (ICOS) in the vaccine-induced group A cells identified in the ASAP-seq dataset. Cells are grouped by their bridge integration-derived labels. **(B)** Violin plots showing the module score of the 197 signature vaccine-induced gene set in the ASAP-seq dataset. The module score is calculated based on gene activity scores, which are derived from scATAC-seq data.

Supplementary Figure 5

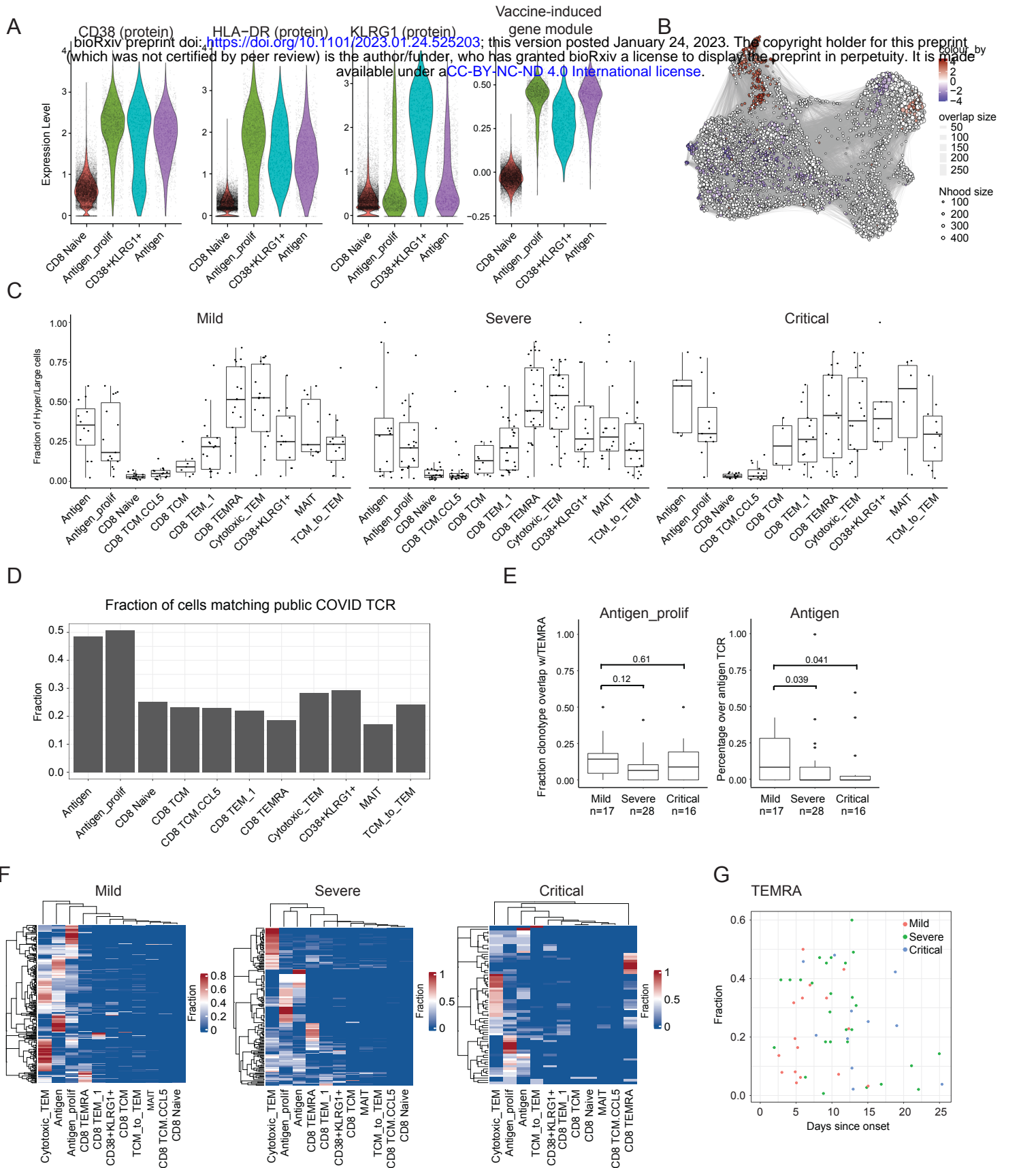
bioRxiv preprint doi: <https://doi.org/10.1101/2023.01.24.525203>; this version posted January 24, 2023. The copyright holder for this preprint (which was not certified by peer review) is the author/funder, who has granted bioRxiv a license to display the preprint in perpetuity. It is made available under aCC-BY-NC-ND 4.0 International license.



Supplementary Figure 5

(A) Flow cytometry data generated during validation of individual dextramer reagents, with the progressive emergence of cells in the Dex+ gate across time points for a single donor. CD8+ cells were used as input. Middle and bottom row show CD38, HLA-DR, and KLRG1 abundance from the parent gate of Dex+CD8+ cells. (B) Boxplots indicate the fraction of cells harboring a hyper- or large-expanded TCR clone in each cluster. Each dot represents one biological sample. (C) Exemplary flow cytometry plots indicating the percentage of cells in CD38+HLA-DR+ gate of a single donor, from a parent gate of CD8+ KLRG1- cells. (D) Boxplot shows the percentage of CD38+HLA-DR+ cells in each donor, as a fraction of the CD8+KLRG1- gate exemplified in (C). Data represents n=4 donors with variable HLA haplotypes. p-value (p=0.0286) was calculated using a Mann-Whitney test.

Supplementary Figure 6



Supplementary Figure 6

(A) Violin plots showing the protein expression of CD38 and HLA-DR, along with the signature gene module score for the vaccine-induced cells, in the COMBAT dataset. (B) Milo analysis of differential abundance changes between healthy and SARS-CoV-2 infected CD8+ T cells groups from the COMBAT dataset. UMAP visualization of the Milo differential abundance testing results. Each node represents a neighborhood. The size of nodes is proportional to the number of cells in the neighborhood. Neighborhoods are colored by their log fold changes for SARS-CoV-2 infected versus healthy groups. Only neighborhoods showing significant enrichment (SpatialFDR < 0.1 and logFC > 2) are colored. (C) Boxplots showing the fraction of cells harboring a hyper or large expanded TCR clone within each cluster. Each dot represents one biological sample. (D) Barplot showing the fraction of cells within each cluster harboring TCR matching SARS-CoV-2 antigens in public databases. (E) Fraction of TCR clonotypes identified in either antigen cells (right) or antigen_prolif cells (left), that are also identified in TEMRA cells. Boxplots show variation across diseased donors. (F) Heatmaps show the distribution of cells harboring expanded antigen-specific TCR sequences among all cell states. Each row corresponds to one expanded clone, clones that are shared between molecular states will exhibit a positive fraction in multiple columns. (G) Scatter plot showing the lack of a potentially confounding correlation between the fraction of CD8 T cells in the TEMRA state, and the sample collection time since onset. Each dot represents one donor and is colored by disease state.